Hybrid surface-enhanced Raman scattering substrate from gold nanoparticle and photonic crystal: Maneuverability and uniformity of Raman spectra

Cheng Yi Wu[1], Chia Chi Huang[2], Jia Sin Jhang[1], An Chi Liu[1], Chun-Chen Chiang[2], Ming-Lung Hsieh[2], Ping-Ji Huang[2], Le Dac Tuyen[1,6], Le Quoc Minh[5], Tzyy Schiuan Yang[2], Lai-Kwan Chau[2], Hung-Chih Kan[1,*] and Chia Chen Hsu[1,3,4,*]

[1]*Department of Physics, National Chung Cheng University, Ming Hsiung, Chia Yi 621, Taiwan*
[2]*Department of Chemistry and Biochemistry, National Chung Cheng University, Ming Hsiung, Chia Yi 621, Taiwan*
[3] *Graduate Institute of Opto-Mechatronics, National Chung Cheng University, Ming Hsiung, Chia Yi 621, Taiwan*
[4]*Department of Photonics, National Sun Yat-sen University, Kaohsiung 804, Taiwan*
[5]*Institute of Materials Science, VAST of Vietnam, Hoang Quoc Viet Road, Hanoi, Vietnam*
[6]*Hanoi University of Mining and Geology, Tu Liem, Hanoi, Vietnam*
**cchsu@phy.ccu.edu.tw; phyhck@ccu.edu.tw*

Abstract: A novel hybrid surface-enhanced Raman scattering (SERS) substrate based on Au nanoparticles decorated inverse opal (IO) photonic crystal (PhC) is presented. In addition to the enhancement contributed from Au nanoparticles, a desired Raman signal can be selectively further enhanced by appropriately overlapping the center of photonic bandgap of the IO PhC with the wavelength of the Raman signal. Furthermore, the lattice structure of the IO PhC provides excellent control of the distribution of Au nanoparticles to produce SERS spectra with high uniformity. The new design of SERS substrate provides extra maneuverability for ultra-high sensitivity sensor applications.

OCIS codes: (160.5293) Photonic bandgap materials; (220.4241) Nanostructure fabrication; (240.6695) Surface-enhanced Raman scattering; (350.4238) Nanophotonics and photonic crystals.

References and Links

1. M. Fleischmann, P. J. Hendra, and A. J. McQuillan, "Raman spectra of pyridine adsorbed at a silver electrode," Chem. Phys. Lett. **26**(2), 163–166 (1974).
2. G. C. Schatz, M. A. Young, and R. P. Van Duyne, "Electromagnetic mechanism of SERS," in Surface-Enhanced Raman Scattering: Physics and Applications (2006), pp. 19–45.
3. S. Chan, S. Kwon, T.-W. Koo, L. P. Lee, and A. Berlin, "Surface-enhanced Raman scattering of small molecules from silver-coated silicon nanopores," Adv. Mater. **15**(19), 1595–1598 (2003).
4. H.-H. Wang, C.-Y. Liu, S.-B. Wu, N.-W. Liu, C.-Y. Peng, T.-H. Chan, C.-F. Hsu, J.-K. Wang, and Y.-L. Wang, "Highly Raman-enhancing substrates based on silver nanoparticle arrays with tunable sub-10 nm gaps," Adv. Mater. **18**(4), 491–495 (2006).
5. L.-Y. Chen, J.-S. Yu, T. Fujita, and M.-W. Chen, "Nanoporous copper with tunable nanoporosity for SERS applications," Adv. Funct. Mater. **19**(8), 1221–1226 (2009).
6. C. R. Yonzon, D. A. Stuart, X. Zhang, A. D. McFarland, C. L. Haynes, and R. P. Van Duyne, "Towards advanced chemical and biological nanosensors-An overview," Talanta **67**(3), 438–448 (2005).
7. L. A. Dick, A. D. McFarland, C. L. Haynes, and R. P. V. Duyne, "Metal film over nanosphere (MFON) electrodes for surface-enhanced Raman spectroscopy (SERS): Improvements in surface nanostructure stability and suppression of irreversible loss," J. Phys. Chem. B **106**(4), 853–860 (2002).
8. S. Kubo, Z.-Z. Gu, D. A. Tryk, Y. Ohko, O. Sato, and A. Fujishima, "Metal-coated colloidal crystal films as surface-enhanced Raman scattering substrate," Langmuir **18**(13), 5043–5046 (2002).
9. L. Lu, I. Randjelovic, R. Capek, N. Gaponik, J. Yang, H. Zhang, and A. Eychmüller, "Controlled fabrication of gold-coated 3D ordered colloidal crystal films and their application in surface-enhanced Raman spectroscopy," Chem. Mater. **17**(23), 5731–5736 (2005).
10. Y. Djaoued, S. Badilescu, S. Balaji, N. Seirafianpour, A.-R. Hajiaboli, R. Banan Sadeghian, K. Braedley, R. Brüning, M. Kahrizi, and V.-V. Truong, "Micro-Raman spectroscopy study of colloidal crystal films of polystyrene-gold composites," Appl. Spectrosc. **61**(11), 1202–1210 (2007).

#117010 - $15.00 USD Received 10 Sep 2009; revised 23 Oct 2009; accepted 1 Nov 2009; published 10 Nov 2009

11. P. M. Tessier, O. D. Velev, A. T. Kalambur, J. F. Rabolt, A. M. Lenhoff, and E. W. Kaler, "Assembly of gold nanostructured films templated by colloidal crystals and use in surface-enhanced Raman spectroscopy," J. Am. Chem. Soc. **122**(39), 9554–9555 (2000).
12. L. Lu, A. Eychmüller, A. Kobayashi, Y. Hirano, K. Yoshida, Y. Kikkawa, K. Tawa, and Y. Ozaki, "Designed fabrication of ordered porous au/ag nanostructured films for surface-enhanced Raman scattering substrates," Langmuir **22**(6), 2605–2609 (2006).
13. D. M. Kuncicky, B. G. Prevo, and O. D. Velev, "Controlled assembly of SERS substrates templated by colloidal crystal films," J. Mater. Chem. **16**(13), 1207–1211 (2006).
14. E. Yablonovitch, "Inhibited spontaneous emission in solid-state physics and electronics," Phys. Rev. Lett. **58**(20), 2059–2062 (1987).
15. S. John, "Strong localization of photons in certain disordered dielectric superlattices," Phys. Rev. Lett. **58**(23), 2486–2489 (1987).
16. C. López, "Materials Aspects of photonic crystals," Adv. Mater. **15**(20), 1679–1704 (2003).
17. H. Míguez, F. Meseguer, C. López, A. Blanco, J. S. Moya, J. Requena, A. Mifsud, and V. Fornés, "Control of the photonic crystal properties of fcc packed submicron SiO_2 spheres by sintering," Adv. Mater. **10**(6), 480–483 (1998).
18. A. Kocabas, G. Ertas, S. S. Senlik, and A. Aydinli, "Plasmonic band gap structures for surface-enhanced Raman scattering," Opt. Express **16**(17), 12469–12477 (2008).
19. J. J. Baumberg, T. A. Kelf, Y. Sugawara, S. Cintra, M. E. Abdelsalam, P. N. Bartlett, and A. E. Russell, "Angle-resolved surface-enhanced Raman scattering on metallic nanostructured plasmonic crystals," Nano Lett. **5**(11), 2262–2267 (2005).
20. N. M. B. Perney, J. J. Baumberg, M. E. Zoorob, M. D. B. Charlton, S. Mahnkopf, and C. M. Netti, "Tuning localized plasmons in nanostructured substrates for surface-enhanced Raman scattering," Opt. Express **14**(2), 847–857 (2006).
21. N. M. B. Perney, F. J. Garcí de Abajo, J. J. Baumberg, A. Tang, M. C. Netti, M. D. B. Charlton, and M. E. Zoorob, "Tuning localized plasmon cavities for optimized surface-enhanced Raman scattering," Phys. Rev. B **76**(3), 035426 (2007).
22. J. Wang, S. Ahl, Q. Li, M. Kreiter, T. Neumann, K. Burkert, W. Knoll, and U. Jonas, "Structural and optical characterization of 3D binary colloidal crystal and inverse opal films prepared by direct co-deposition," J. Mater. Chem. **18**(9), 981–988 (2008).
23. C. Y. Wu, N. D. Lai, and C. C. Hsu, "Rapidly self-assembling three-dimensional opal photonic crystals," J. Korean. Phys. Soc. **52**(5), 1585–1588 (2008).
24. K. Kwon, K. Y. Lee, Y. W. Lee, M. Kim, J. Heo, S. J. Ahn, and S. W. Han, "Controlled synthesis of icosahedral gold nanoparticles and their surface-enhanced Raman scattering property," J. Phys. Chem. C **111**(3), 1161–1165 (2007).

1. Introduction

Surface-enhanced Raman scattering (SERS) has been the key for developing ultra-high sensitivity sensors for biochemical molecules since its discovery in 1974 [1]. For practical sensor design, Au or Ag nanoparticle decorated surfaces are the first candidates for SERS substrates. The idea is simply to utilize the SERS effect from nanoparticles, which results from the electric field enhanced by the localized surface plasmon excited by the incident light and its interaction with the individual molecules attached to the surface [2]. For practical applications besides high sensitivity an ideal sensor should also produce SERS spectra with uniformity and reproducibility. By definition, uniformity means that the quality of the Raman spectra should be independent of the locations on the substrate where they are measured. Normally the SERS measurement could be performed with a focused beam spot for excitation. The diameter of the beam spot could be tens of micrometers and the resulting spectra is an average of the signal from the illuminated area. This implies that the uniformity could be achieved by further engineering on the substrate to control the size and the aggregation of the nanoparticles at much smaller scale on the surface. Among the numerous designs reported in the literature, patterning the substrate with random or periodical structures seems to be the major approach. It ranges from the use of random porous structure [3–5] to self-assembled periodical structures [6–13]. Among them, the periodically patterned SERS substrates that consist of metallic-dielectric nanostructures in fact bear the vary nature of the photonic crystals (PhC) or plasmonic crystals, in which a photonic bandgap (PBG) [14–17] or plasmonic bandgap [18–21] may exist in some directions of light propagation.

It is well known that the PBG of a PhC provides means of manipulating and controlling the flow of light. Therefore, when the structure of PhC is present in a SERS substrate, similar effects can be expected on the flow of the incident light or that of the SERS signals. For instance, by carefully aligning the PBG of a PhC substrate with peaks in the Raman spectra

#117010 - $15.00 USD Received 10 Sep 2009; revised 23 Oct 2009; accepted 1 Nov 2009; published 10 Nov 2009

one can selectively make some Raman signal to be reflected from the substrate and some to propagate through, leading to selectivity in the detection of the SERS signal. Some studies about the application of plasmonic bandgap effect to enhance SERS signals have been reported previously [18–21]. However, at present there are only a few investigations regarding using PBG effect on SERS signals.

In this paper we demonstrate the maneuverability as well as the superb uniformity of SERS spectra from a substrate that combines the optical property of Au nanoparticle and the feature of the PBG of an inverse opal (IO). We first present a novel and simple method to fabricate the IO PhC on the substrate with a commercially available photoresist, followed by the chemical process to decorate Au nanoparticles on the top layer of the IO PhC [22]. We then present our investigation on the effect of PBG of the substrate on the SERS signals to show that SERS signals are further enhanced when the wavelength of Raman signal aligned with the PBG of the Au nanoparticle decorated IO substrate.

2. Experiments

To fabricate the Au nanoparticle decorated IO PhC substrate, the SiO_2 opal template was first fabricated with a thermal-assisted cell method [23], and the opal template obtained consists of large size domains and has a smooth top surface. The SU-8 (MicroChem Inc.) IO template was then fabricated by first filling SU-8 photoresist in the free space in the SiO_2 opal template with infiltration method followed by the removal of SiO_2 from the SU-8 filled opal. We then decorated the top layer of the IO with Au nanoparticles, which were prepared by the reduction of $HAuCl_4 \cdot 4H_2O$ with sodium citrate. The average diameter of Au nanoparticles used in our study is 30 nm with a standard deviation less than 5 nm.

2.1 The gold nanoparticles *decoration process*

Figure 1 shows the initial, intermediate, and final surface chemical composition of the SU-8 IO through the chemical procedures used for Au nanoparticle deposition in four steps. Panel (A) shows the initial molecular composition of the SU-8 IO surface. The first step was to hydrolyze the IO SU-8 scaffold surfaces with 0.1 M sodium hydroxide (NaOH) for 1 hour to convert their epoxy functional groups (as shown in Panel (A)) to carboxylic acid groups as shown in panel (B). The next step was to oxidize the hydrolyzed SU-8 surfaces with 0.1 M strong oxidant potassium chromate ($K_2Cr_2O_7$) for 1 hour to produce the surface molecular composition shown in panel (C). In the third step, the oxidized SU-8 surface was further modified to contain thiol (SH) functional groups with the mixture of 1-ethyl-3-(3-dimethylaminopropyl)-carbodiimide ($C_8H_{17}N_3 \cdot HCl$), N-hydroxysuccinimide (NHS, $C_4H_5NO_3$) and cystamine dihydrochloride ($C_4H_{12}N_2S_2 \cdot 2HCl$) in 2-(4-(2-hydroxyethyl)-1-piperazinyl)-ethanesulfonic acid buffer solution (pH = 7.5) for 2 hours, and the resulted surface structure is shown in panel (D). In the final step, Au nanoparticles covered with citrate anions were attached to the IO SU-8 scaffold surfaces via -SH groups, as shown in panel (E). To avoid the contamination, the SU-8 IO templates were rinsed with de-ionized water after each step. Due to the fact that the SU-8 surface is hydrophobic, ultrasonic treatment was applied for 5 minutes in each processing step to facilitate the reaction. The surface density of Au nanoparticle on SU-8 IO templates was controlled by varying the ultrasonic and the soaking time in the final step. In this report, we vary the lattice constant of the IO substrate as well as the surface density of the Au nanoparticle to investigate the effect of the PBG on the SERS signals, and for control experiment we used a Au film coated glass substrate and a Au nanoparticle decorated flat SU-8 surface.

#117010 - $15.00 USD Received 10 Sep 2009; revised 23 Oct 2009; accepted 1 Nov 2009; published 10 Nov 2009

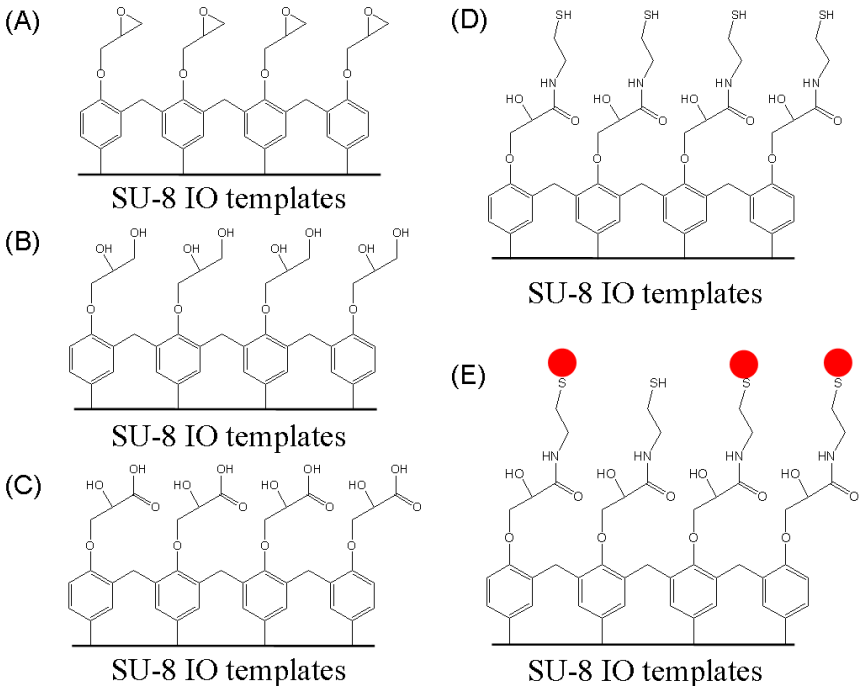

Fig. 1. The chemical modification process of gold nanoparticles on SU-8 IO templates.

2.2 SERS speactra and optical reflection spectra measurement

Prior to the Raman spectra measurement, all substrates were immersed in an ethanol solution containing the probe molecules 4-NBT (10^{-2} M) for 2 minutes, and the 4-NBT molecules replaced the citrate anions and directly attached to the Au nanoparticles. A He-Ne laser (Spectra Physics) with 36 mw output power at 632.8 nm wavelength was used to excite the molecules. A laser filter (Chroma Z633/10 ×) was used to remove other residual plasma lines from the incident beam, which was then focused by a 20 × objective lens (NA = 0.4) onto the sample. The back-scattered photons were collected with the same objective lens. A plano-convex lens was used to focus the scattered photons onto a fiber, which further transmitted the scattered photons to a spectrometer. A Raman filter (Omega XR3303) was used before the plano-convex lens to block the excitation laser. The SERS spectra were detected by an air-cooled charge-coupled device (CCD) camera (Andor DU401-BV) at –50 °C. The integration time for each SERS spectrum was set to 15 seconds.

The optical reflection spectra were measured with a system consisted of a tungsten lamp white light source and an Ocean Optics S2000 UV-visible fiber optic spectrometer. The incident white light was collimated with a beam-expanding system, and split into two beams for the reflection spectrum measurement. The beam diameter was controlled to be within 1 mm [23].

3. Results and discussion

Figures 2(A) to 2(C) show the field-emission scanning electron microscopy (FESEM) images of Au nanoparticles on a flat SU-8 surface (Fig. 2(A)) and those on IO templates (Figs. 2(B) and 2(C)). For both type of substrates, Au nanoparticles attached to the surface randomly. For flat substrate, the number densities σ (μm^{-2}) of Au nanoparticles on the substrate surface is determined by simply counting the number of Au nanoparticles in the FESEM images over a fixed area.

#117010 - $15.00 USD Received 10 Sep 2009; revised 23 Oct 2009; accepted 1 Nov 2009; published 10 Nov 2009

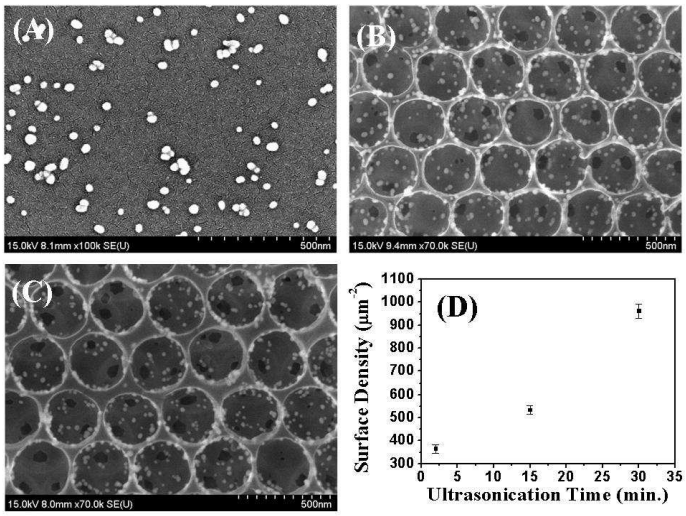

Fig. 2. The FESEM images of Au nanoparticles on (A) flat SU-8 surface with number density σ = 93 μm^{-2}, (B) IO substrate SU-8 IO-II (Λ = 317 nm) with σ = 315 μm^{-2}, and (C) IO substrate IO-III (Λ = 337 nm) σ = 365 μm^{-2}. (D) The number density of Au nanoparticle on substrate IO-II as a function of ultrasonification time in last step of the chemical process.

For the IO template, according to the side view SEM image of the IO decorated with Au nanoparticles, they mostly attached to the top layer, and only few of them goes beyond the top layer. Therefore, for the discussion below we ignore the few nanoparticles beyond the top layer. To estimate the average number density of Au nanoparticles on the surface, we count the number of particles visible in the top view SEM images and dividing it with the total area, i.e. the area of the top grid and that of the spherical bottom seen in each void. We assume the same number density for the region invisible in the SEM images. Figure 2(D) shows the typical ultrasonification time (in the last processing step) dependence of σ for an IO substrate. It basically increases monotonically although not linearly with ultrasonification time. With this general trend we control the total number of Au nanoparticles deposited on the templates.

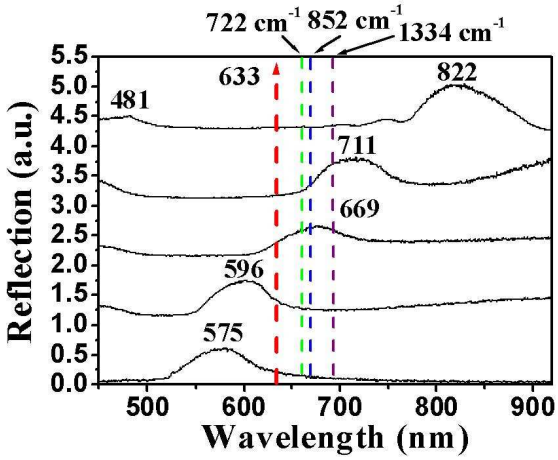

Fig. 3. The reflection spectra of SU-8 IO SERS substrates at normal incidence. The vertical dashed lines indicate the wavelength of the incident light (633nm) and those of three peaks in the Raman spectra shown in Fig. 4(a), whose wave number shifts are as labeled.

#117010 - $15.00 USD Received 10 Sep 2009; revised 23 Oct 2009; accepted 1 Nov 2009; published 10 Nov 2009

Figure 3 shows the reflection spectra at normal incidence measured from our SU-8 IO substrates with varying lattice constant after the decoration of Au nanoparticle and the coating of the 4-NBT probe molecules. The lattice constant for each substrate follows: Λ = 307 nm for substrate labeled "IO-I", Λ = 317 nm for "IO-II", Λ = 337 nm for "IO-III", Λ = 366 nm for "IO-IV", and Λ = 395 nm for "IO-V". The broad reflectivity peak in each plot is the signature of the PBG of the SU-8 IO substrates at normal incidence. For substrate IO-I (σ = 560 μm^{-2}) the reflectivity peaked at the wavelength of at 575 nm, 596 nm for substrate IO-II (σ = 534 μm^{-2}), 669 nm for substrate IO-III (σ = 582 μm^{-2}), 711 nm for substrate IO-IV (σ = 594 μm^{-2}), and 822 nm for substrate IO-V (σ = 584 μm^{-2}). The full width of half maximum (FWHM) of the reflectivity peaks are 64, 62, 67, 69, and 81 nm, for substrate IO-I, IO-II, IO-III, and IO-IV, IO-V, respectively. The decoration of Au nanoparticle and the coating of the SERS probe molecules on an IO substrate only have minor effect on its optical property. For a fixed Λ, the reflection peak red shifts slightly with increasing σ, reaching a total shift of ~10 nm for the maximum surface density of Au nanoparticles used in this experiment. No significant broadening of the reflection peak is observed as σ increases. The vertical dash lines denotes the laser excitation wavelength (633 nm), and wavelengths of three peaks in the SERS spectra shown in Fig. 4, whose wave number shifts are indicated by the labels.

Figure 4(A) compares the Raman spectra from the 4-NBT probe molecules (shown in the inset) coated on the control sample, i.e. the Au thin film coated on a glass surface (substrate I) and a flat SU-8 surface decorated with Au nanoparticles (substrate II), and the Au nanoparticle decorated SU-8 IO substrates (IO-I, IO-II, IO-III, IO-IV, and IO-V). The spectral peaks results from the Raman scattering of the incident light attributed from the 4-NBT molecules, not from the Au nanoparticles.

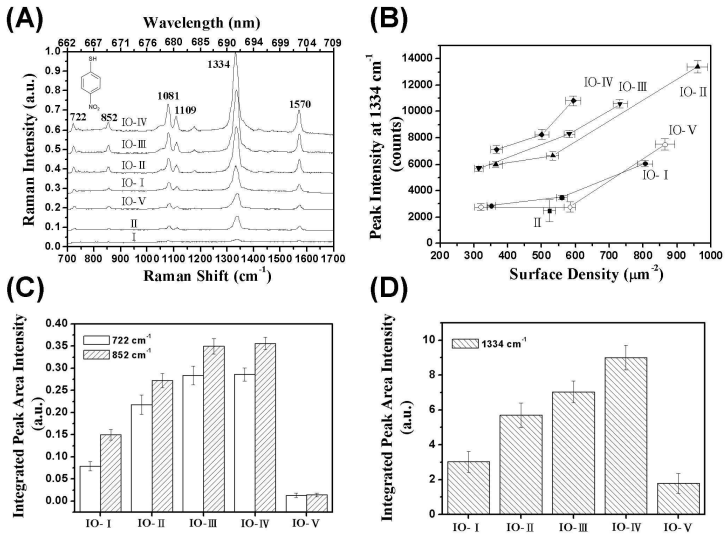

Fig. 4. (A) Raman spectra from (I): gold thin film (thickness = 32 nm) on a glass substrate, (II): a flat SU-8 surface decorated with Au nanoparticles (σ = 524 μm^{-2}), and SU-8 IO SERS substrates with different lattice constants; (IO-I): (Λ = 307 nm, σ = 560 μm^{-2}), (IO-II): (Λ = 317 nm, σ = 534 μm^{-2}), (IO-III): (Λ = 337 nm, σ = 582 μm^{-2}), (IO-IV): (Λ = 366 nm, σ = 594 μm^{-2}), (IO-V): (Λ = 395 nm, σ = 584 μm^{-2}). The inset shows the chemical structure of 4-NBT. (B) The SERS peak intensities at 1334 cm^{-1} as a function of σ for substrate II and the five SU-8 IO substrates. (C) and (D) show the block chart of SERS integrated peak area intensities comparison at 722, 852 and 1334 cm^{-1} from the same IO substrates in (A).

The general features of the SERS spectra obtained here agree with the results reported previously [24]. The higher peak intensities in the Raman spectrum II compared to those in spectrum I indicate the enhancement from the localized surface plasmon excited on the Au

#117010 - $15.00 USD Received 10 Sep 2009; revised 23 Oct 2009; accepted 1 Nov 2009; published 10 Nov 2009

nanoparticles with the incident light. Therefore the enhancement observed in our Raman spectra first comes from the Au nanoparticles decorated on the substrate. Due to the 3-dimentional nature of the IO substrates, the number of Au nanoparticles illuminated by the incident light per projected unit area is larger than that of the flat substrate, assuming that they have the same surface number density σ and the distribution is fairly uniform. For our IO substrates the increment could be a factor of two, which is about the same for all IO substrate. This leads to higher Raman signal intensity for the IO substrate compared to that from the flat substrate. Figure 4(B) shows the peak intensities at 1334 cm^{-1} wave number shift in the Raman spectra measured from SU-8 IO substrates and that from substrate II as a function of σ. For a given substrate, the peak intensity increases with σ. For a fixed σ, the peak intensity varies with the periodicity of IO substrate with maximum occurring around that of substrate IO-IV. Figures 4(C) and 4(D) further compares the peak area intensities at 722 cm^{-1}, 852 cm^{-1} and 1334 cm^{-1} Raman shifts measured from the spectra of the IO substrates in Fig. 4(A). As indicated in Fig. 3 the wavelengths of the 722 cm^{-1}, and 852 cm^{-1} Raman shifts locate within the range of the PBG of substrate IO-III, and that of the peak at 1334 cm^{-1} Raman shift in range of PBG of substrate IO-IV. Therefore it is easy to see a general trend for the intensities shown here. When the SERS peak wavelength is within the range of the PBG, the substrate produces higher intensity. By the same token, for substrate IO-I and IO-V, their PBGs are distant from the wavelengths of these three peaks, thus producing lower peak intensities. Substrate IO-II seems to be the transition between the two extremes, thus producing Raman spectra with intermediate intensities. This clearly demonstrates that Raman signals enhanced by the Au nanoparticles are affected by the IO substrates due to the presence of PBG. It can be reasoned that when the wavelength of the Raman signal coincides with the PBG, the PhC IO substrate forbids the Raman signal to propagate downward. Instead, it is Bragg-reflected from the substrate in the normal direction, in which our detector was positioned, leading to the IO periodicity dependence of the peaking intensity shown here. This clearly demonstrates the selectivity in the further enhancement of SERS signal with a PhC substrate, when its PBG is specially designed to manipulate the flow of the Raman signal.

Figures 5(A) and 5(B) compares the uniformity of the SERS spectra obtained from the PhC substrate IO-IV (σ = 501 μm^{-2}) and those from a flat SU-8 substrate decorated with Au nanoparticle, i.e. substrate II (σ = 98 μm^{-2}). The nine spectra shown in each panel were obtained from the same sample over a surface area of 1 × 1 cm^2. The uniformity of the SERS spectra from the PhC substrate IO-IV obviously excels those from the flat substrate decorated with Au nanoparticles. The standard deviations of SERS peaks between 700 - 1600 cm^{-1} is on the order of 15% for the substrate IO-IV, and over 40% for the substrate II, which is typical for this type of substrate. This demonstrates that the skeleton structure provided by the IO PhC allows an excellent control of the distribution of Au nanoparticles used for SERS to produce spectra with high uniformity.

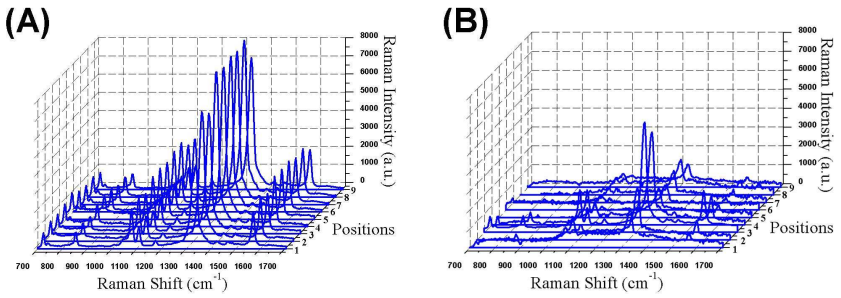

Fig. 5. (A) and (B) show the spectra of 4-NBT probe molecules on the IO-IV sample (σ = 501 μm^{-2}) and on the sample II (σ = 98 μm^{-2}), respectively.

#117010 - $15.00 USD Received 10 Sep 2009; revised 23 Oct 2009; accepted 1 Nov 2009; published 10 Nov 2009

4. Conclusions

In conclusions, we present a novel design of the SERS substrate for practical sensor application, which combines the optical property of Au nanoparticles and that of the IO PhC. We first demonstrate that by proper choice of the lattice constant the PBG of the IO PhC substrate can selectively further enhance a desired Raman signal that has been enhanced by Au nanoparticles in the first place. Secondly, the lattice structure of the IO provides an excellent substrate to control the uniformity in the distribution of nanoparticles attached to the substrate through the chemical procedure we developed. This leads to the superb uniformity of the SERS spectra obtained. We foresee that besides enhancement of the Raman signal, the maneuverability of the signal flow provided by Au nanoparticle decorated IO substrate allows versatile sensor design for SERS application.

Acknowledgements

We acknowledge the financial support by the National Science Council of the Republic of China, Taiwan (Contract Nos. NSC 98-2112-M-194-008-MY3, NSC 98-2627-E-194-001, NSC-96-2112-M-194-014-MY3).

#117010 - $15.00 USD Received 10 Sep 2009; revised 23 Oct 2009; accepted 1 Nov 2009; published 10 Nov 2009